



Vibration Monitoring of Paper Mill Machinery

Written By

James C. Robinson, Technical Consultant, IMI division of PCB Piezotronics

Curated By

Meredith Christman, Product Marketing Manager, IMI division of PCB Piezotronics

VIBRATION MONITORING OF PAPER MILL MACHINERY

Article by:

James C Robinson, Technical Consultant, IMI division of PCB Piezotronics

Curated by:

Meredith Christman, Product Marketing Manager, IMI division of PCB Piezotronics

INTRODUCTION

Paper mills are composed of several large sections of machinery. Because the operation of each section is essential for the overall operation of the mill, planned downtime of any one section is inconvenient and unplanned downtime can be catastrophic.

The objective of this paper is to demonstrate a wide variety of fault types and the importance of employing proper sensors and analysis tools. Particular emphasis is placed on vibration monitoring employing accelerometers on paper mill equipment.

SECTION 1: SENSOR SELECTION AND MOUNTING

Paper Plant Overview and Potential Faults: Prior to selecting sensors and addressing their mounting on paper industry machinery, it will first be beneficial to remind ourselves of the machinery employed and the characteristics of the vibration signature which can be expected from faults common to that machinery. The product flow is presented in Figure 1.

There are a variety of faults that can occur in this industrial equipment. For example, if there is a crack in a gear, it will likely introduce a slight speed change when the defective tooth enters the load zone. This leads to impacting every time that tooth enters into its load carrying responsibility (typically once per revolution of that gear). Now consider a situation where there is a lack of sufficient lubrication for the gear teeth going into and out of the load zone. This leads to friction between the teeth with the maximum activity typically occurring twice per tooth mesh (once on the addendum and once on the dedendum). Of course, both friction and impacting can also occur within the bearings. In bearings, impacting will generally be periodic and friction generally non-periodic (random).

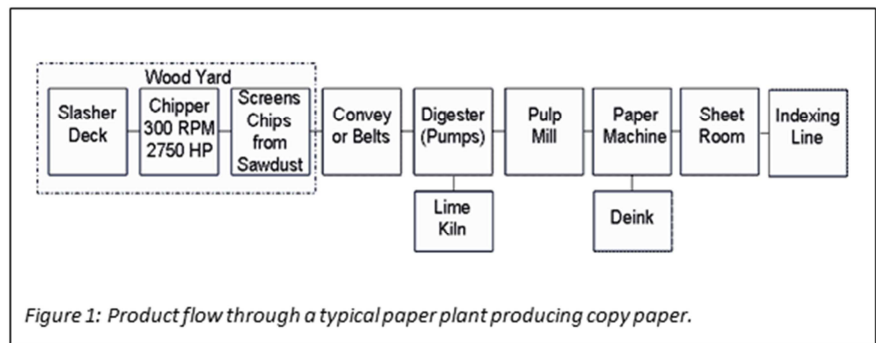


Figure 1: Product flow through a typical paper plant producing copy paper.

When friction or impacting does occur, a short burst of energy (stress wave activity) is emitted in the form of vibration and travels away from the initiation site through the metal at the speed of sound.¹ The stress waves introduce a short-term ripple on the surface of the frame metal that is detectable with an accelerometer sensitive to the frequency within the stress wave packet. The frequencies within the stress wave packets

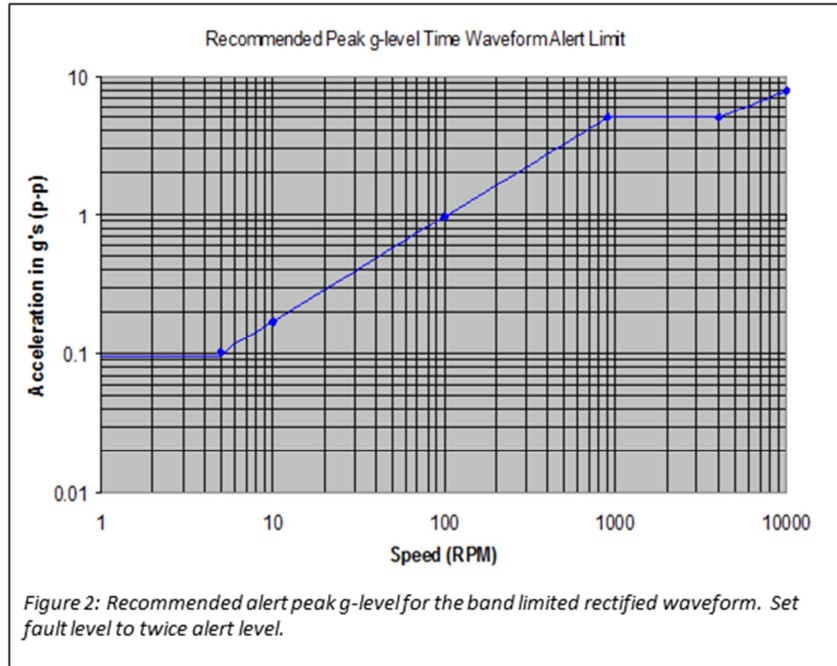
¹James C Robinson, "High Frequency Vibration Analysis." Proceedings of Vibration Institute 2009 Annual Meeting.

generally are in the 1-20 kHz range. Impacting between two specific components generates a packet of energy whose center frequency is typically less than that generated from the same components undergoing friction.

In addition to the relatively high frequencies present in the stress wave packets generated by friction and impacting, the lower frequencies generated by faults such as misalignment and balancing issues must also be captured and analyzed. These stress wave packets contain frequencies in one of the following two ranges:

- About 0.3 times running speed to about 3.25 times the gear meshing frequency.
- About 0.3 times running speed to about 50 times running speed.

The analysts in the plant referenced in the following case studies rely heavily on the audio from the sensor-driven headphones. The audible level of the signal from the sensor and the peak g-level from the band-limited rectified waveform (acquired using the PeakVue™² methodology) are heavily relied on for severity assessment. The recommended alert/fault levels for the PeakVue™ waveform are presented in Figure 2. The levels (which are speed-dependent) presented in Figure 2 are alert levels; it is recommended that the fault level be set at twice the alert level.



ICP® Accelerometer Use: The most common sensor type employed in vibration analysis on paper mill machinery are ICP® accelerometers with a sensitivity of 100 mV/g, a resonant frequency in the 25 kHz range and a noise floor of approximately 100 µg/√Hz at 1 Hz (or less). IMI Model 603C01 (top exit with ¼-28 female mounting thread) would be an example of an ideal model. The specification sheet for the accelerometer typically specifies the sensitivity is nominally flat to within 3dB from a fraction of 1 Hz to 10 kHz. See Figure 3 for an example of the characteristic compliance of Model 603C01.

The implicit assumption is that the sensor is attached to a clean flat surface with a stud at a specified torque. Because stud mounting is both expensive and time consuming, its requirement encourages sparse data acquisition. The analyst will often turn to a much simpler means of attaching the sensor to the surface, such as using a two-rail magnet placed on a curved surface with the sensor attached to the magnet. This approach will often lead to not capturing the higher frequencies associated with impacting or friction.

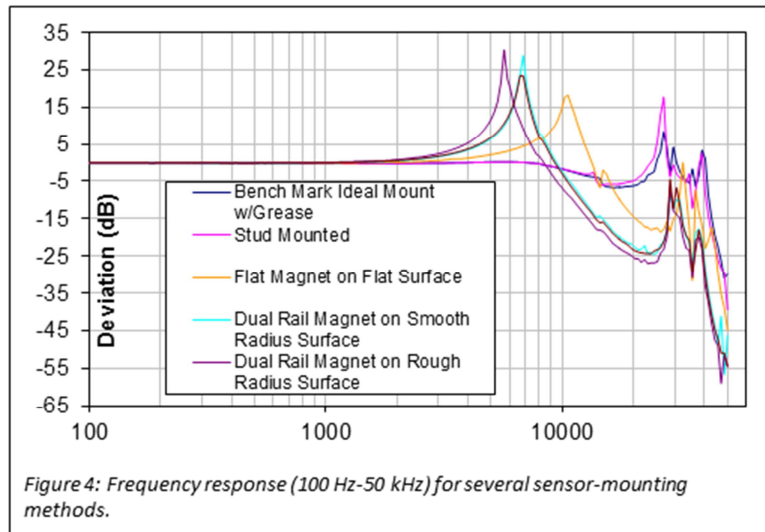
Model Number	INDUSTRIAL ICP® ACCELEROMETER	
603C01		
Performance	ENGLISH	SI
Sensitivity (10 Hz)	100 mV/g	10.2 mV/(m/s ²)
Measurement Range	± 50 g	± 490 m/s ²
Frequency Range (± 3 dB)	30 to 600,000 cpm	0.5 to 10,000 Hz
Resonant Frequency	1500 kcpm	25 kHz
Broadband Resonator (1 to 10,000 Hz)	250 µg	34.34 µm/s ²
Non-Linearity	± 1 %	± 1 %
Transverse Sensitivity	± 7 %	± 7 %
Environmental		
Overload Limit (Shock)	5000 g pk	49,050 m/s ² pk
Temperature Range	-65 to +250 °F	-54 to +121 °C
Temperature Response	See Graph	See Graph
Enclosure Rating	IP68	IP68
Electrical		
Settling Time (within 1% of bias)	≤ 2.0 sec	≤ 2.0 sec
Discharge Time Constant	3.0 sec	3.0 sec
Excitation Voltage	18 to 28 VDC	18 to 28 VDC
Constant Current Excitation	2 to 20 mA	2 to 20 mA
Output Impedance	<150 ohm	<150 ohm
Output Bias Voltage	8 to 12 VDC	8 to 12 VDC
Spectral Noise (10 Hz)	8 µg/√Hz	78.5 µm/s ² /√Hz
Spectral Noise (100 Hz)	5 µg/√Hz	49.1 µm/s ² /√Hz
Spectral Noise (1 kHz)	4 µg/√Hz	39.2 µm/s ² /√Hz
Electrical Isolation (Case)	>10 ⁶ ohm	>10 ⁶ ohm
Physical		
Size (Hex x Height)	1 1/16 in x 1.65 in	18 mm x 42.2 mm
Weight	1.6 oz	51 gm
Mounting Thread	1/4-28 Female	No Metric Equivalent
Mounting Torque	2 to 5 R-lb	2.7 to 6.8 N-m
Sensing Element	Ceramic	Ceramic
Sensing Geometry	Shear	Shear
Housing Material	Stainless Steel	Stainless Steel
Sealing	Welded Hermetic	Welded Hermetic
Electrical Connector	2-Pin MIL-C-5015	2-Pin MIL-C-5015
Electrical Connector Position	Top	Top

Figure 3: Model 603C01 specifications illustrate the recommended characteristics of an ICP® accelerometer used in paper machinery vibration monitoring and/or analysis.

² Jim Crowe and Jim Robinson, "An Overview of the PeakVue™ Methodology Demonstrated with Case Studies." 30th Annual Meeting Proceedings of Vibration Institute, Louisville, KY, pp. 149-158.

To explore the impact that sensor mounting has on the sensor frequency response, frequency response data was captured (presented in Figure 4) for a sensor that was:

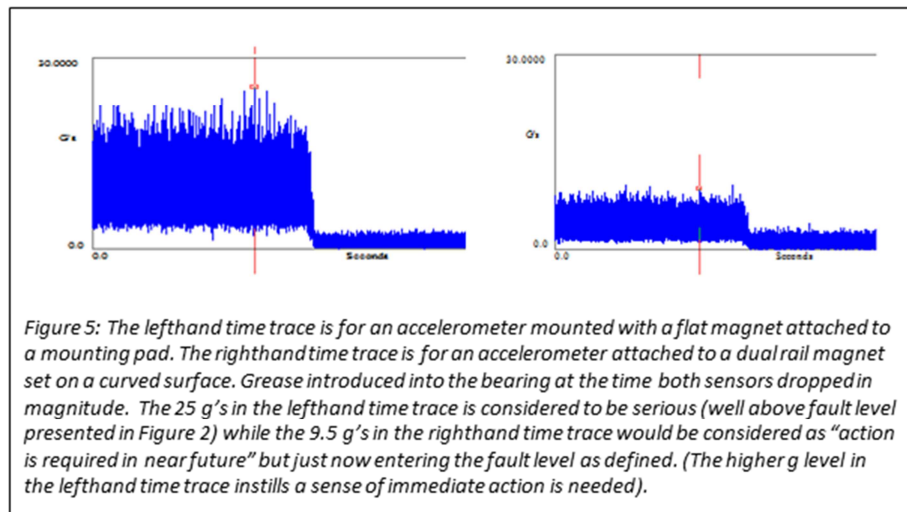
- Mounted with a stud with grease on a flat dry surface.
- Mounted with a stud without grease on a flat dry surface.
- Mounted with a flat magnet on a flat clean surface.
- Mounted with a dual-rail magnet mounted on smooth curved surface.
- Mounted with a dual-rail magnet mounted on rough curved surface.
- Mounted with a dual-rail magnet mounted on painted curved surface.



For faults that manifest themselves in the frequency range of less than 2 kHz such as alignment, unbalance and looseness, the results would be independent of how the sensor is mounted. For faults identified with higher frequencies (impacting and friction), the results would be highly dependent to how the sensor is mounted ranging from no response to distorted response.

Of course, the best way to mount would be stud-mount with a specified torque. This could get expensive as it requires a dedicated accelerometer at every measurement point. An acceptable alternative mounting would be to use a flat magnet placed on a flat smooth surface such as a mounting pad. The flat magnet approach to all measurements points combined with stud mounting the sensor in radial direction on the inboard and outboard ends would be a recommended method for sensor mounting.

To illustrate the type of effect that sensor mounting can have on friction activity, data is presented in Figure 5 from a case where it was known that bearing lubrication was needed. In the lefthand time trace, the sensor was mounted using a flat magnet attached to a flat smooth surface. A second set of data on the righthand time trace was acquired from a sensor attached to a curved surface via a dual-rail magnet. Both time traces were taken at the same time using a two-channel data collector. The bearing was lubricated (greased) at the time the sudden level of noise decreased.



Data Analysis: The analysts' methodology highly relied on PeakVue™ and the autocorrelation coefficient. The below text provides an overview of the analysis methodology.

In normal vibration analysis, the analog signal originating in the sensor is passed through a low-pass filter (anti-aliasing filter) and sampled at a rate of 2.56 times the analysis bandwidth (F_{max}) specified by the analyst. A block of data equal to 2.56 times the number of lines specified by the analyst is acquired. Upon completion of acquiring the time waveform, the spectral data are computed by transforming the time block of data to the spectra data block.

The PeakVue™³ methodology differs by:

- 1. Passing the analog signal from the sensor through a user- specified high-pass filter (greater or equal to the user specified F_{max}).*
- 2. Passing analog (equivalent) signal through a low-pass filter set at 40 kHz and sample the resultant analog signal at a constant rate corresponding to a 40 kHz F_{max} or 2.56 times 40,000, which is 102,400 s/s.*
- 3. Decimating the digital string of data from step 2 by a factor of 40,000/ F_{max} saving the absolute peak value out of each decimation step to a digital block of length 2.56 times the user-specified number of lines. Continue until the digital block of data is filled (this is the PeakVue™ waveform).*

The PeakVue™ waveform is generally transformed into the spectral domain (employing the same method used for the normal vibration waveform) for the purpose of identifying significant periodic activity.

In addition to the generation of the PeakVue™ spectral data from the PeakVue™ waveform, it frequently is beneficial to generate the autocorrelation coefficient function data⁴ from the same PeakVue™ waveform. Assume the PeakVue™ waveform contains N data points; the first step is to shift the PeakVue™ waveform to where the average value for the waveform is zero. Let the elements in the shifted waveform be represented by x_i for $i = 1 \dots N$. Then the autocorrelation functions are computed by the equation:

$$R(\tau_j) = \frac{2}{N} \sum_{i=1}^{N/2} x_i x_{i+j}$$

where

$$\begin{aligned} j &= 0, 1 \dots N/2 \\ x_i &= x(t = i\Delta t), \quad i = 1, 2, \dots, N/2 \\ x_{i+j} &= x(t = [i+j]\Delta t), \end{aligned}$$

The most common vibration sensors employed on industrial machinery used in the paper industry are accelerometers. If a fault is present that is generating stress wave activity within the machine being monitored, that energy will be transmitted to the outer housing through the bearings. An accelerometer fastened to the outer surface in the proximity of that bearing would capture the stress wave activity providing the accelerometer has sufficient bandwidth and sensitivity. If the bearing is a sleeve bearing, significant attenuation will occur to the stress waves in coupling across the gap from inner race to outer

³ PeakVue™ is an analysis methodology offered by Emerson Process Management.

⁴ James C. Robinson, "Autocorrelation as a Diagnostic Tool." 30th Annual Meeting Proceedings of Vibration Institute, Louisville, KY, pp. 79-92.

race and thus may not be sufficient for capture by the sensor. A proximity probe lacks sufficient sensitivity for the relatively high frequency stress wave activity. Fortunately, a significant fraction of the industrial machinery employed in the paper industry employs anti-friction rolling element bearings.

There will be $N/2$ elements in the autocorrelation function. The first element in the autocorrelation function is the mean square of the shifted waveform. The mean square has wide variability; hence it would be difficult to develop this function as a general diagnostic tool.

The normalized autocorrelation function (called the autocorrelation coefficient) is computed from

$$A(\tau_j) = \frac{R(\tau_j)}{R(\tau_0)}$$

This function is independent of the variability of the variance (mean square value).

For a signal, which is representative of a random process, the autocorrelation coefficient will have a value approaching zero for all but the first data point (which is 1.0). For a signal that is periodic with little or no noise, the autocorrelation coefficient will approach ± 1.0 at a time corresponding to the period of the periodic event. For a signal that has a mixture of random and periodic activity, the random signal component will be near zero and hence the non-zero component will be from the periodic component. Taking the square root of the remaining periodic component tells the analyst about what fraction of the signal is from the periodic activity.

The autocorrelation procedure is an averaging (scalar) process with no phase information. It is similar to the more common synchronous averaging (which is vector averaging) process without phasing. The beneficial features of the autocorrelation coefficient function are evident where the spectral data has its main weakness such as

- Clear indicator of random data
- Identifying low frequency periodic events in the waveform.
- Separating the fundamental frequency from many harmonic family activity, etc.

SECTION 2: DEINK SECTION CASE STUDIES

Case Study 1: When acquiring routine surveillance velocity spectral data on a pulp screw inboard motor, an audible clicking noise was heard. This noise prompted the acquisition of additional band-limited vibration data (1 kHz to 40 kHz) employing the PeakVue™ methodology. The PeakVue™ spectral data and waveform are presented in Figure 6. The peak g level in Figure 5 is 1.25 g's, which is low compared to the recommended alert level of 5 g's. The recommended action to take was to simply note that an obvious outer race fault was present. No other specific action was recommended at the time since the peak g level of 1.25 g's was well below the recommended alert level of 5 g's. The signature seen in Figure 6 (low g level with the spectra clearly indicating a bearing race fault) is typically encountered when fatigue cracking is present that starts in the bearing race interior. The fatiguing will continue until the cracks reach the inner or outer surface of

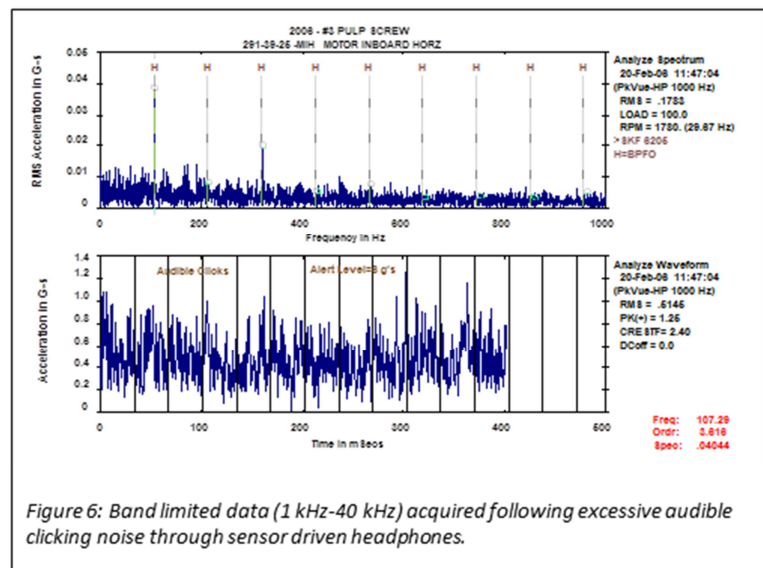


Figure 6: Band limited data (1 kHz-40 kHz) acquired following excessive audible clicking noise through sensor driven headphones.

the race during which time the peak g level will trend upward in magnitude. If the bearing was removed for replacement at the time of measurement collection, there may not have been any visible evidence of a bearing fault as fatigue cracking may not have propagated to the outer surface of the bearing race.

Case Study 2: On a routine vibration data acquisition, a large amount of noise was detected in the audio headphones on a disperser inboard motor. This triggered the capture of rectified band-limited data (1 kHz-40 kHz).

The spectra and waveform data are presented in Figure 7. The peak g level in Figure 7 is 10 g's, which is the recommended fault level. The normal recommended action to take when the fault level is reached is to:

- Monitor more frequently.
- Start planning for corrective action regarding the fault.

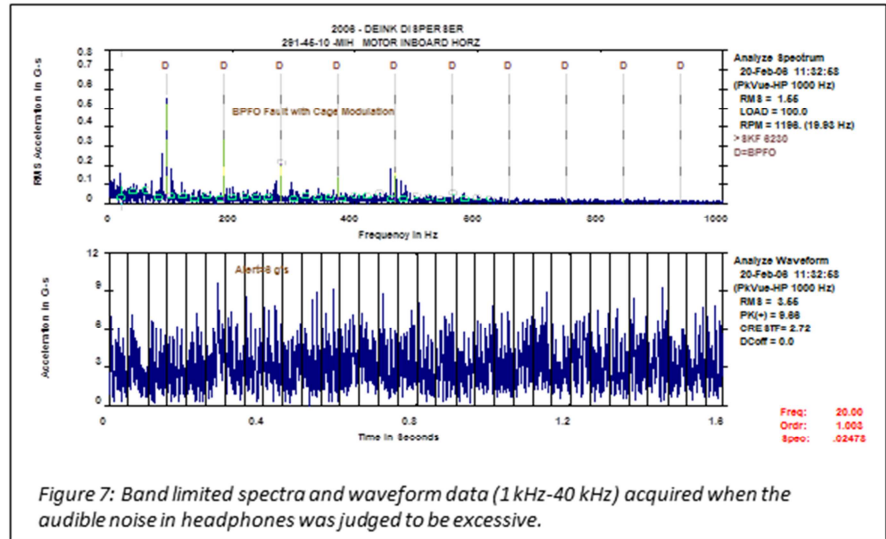


Figure 7: Band limited spectra and waveform data (1 kHz-40 kHz) acquired when the audible noise in headphones was judged to be excessive.

The obvious fault identified in Figure 7 is an outer race fault, also known as ball pass frequency of outer (ring) (BPFO). In addition to the BPFO fault identified in Figure 7, there was a probable second fault identified by the side bands to the first BPFO spectra data point that was due to modulation of the BPFO fault. This is best seen in the autocorrelation coefficient data presented in Figure 8. The data presented in Figure 7 was computed from the waveform presented in Figure 7. The horizontal axis in Figure 8 is in milliseconds. The vertical bars

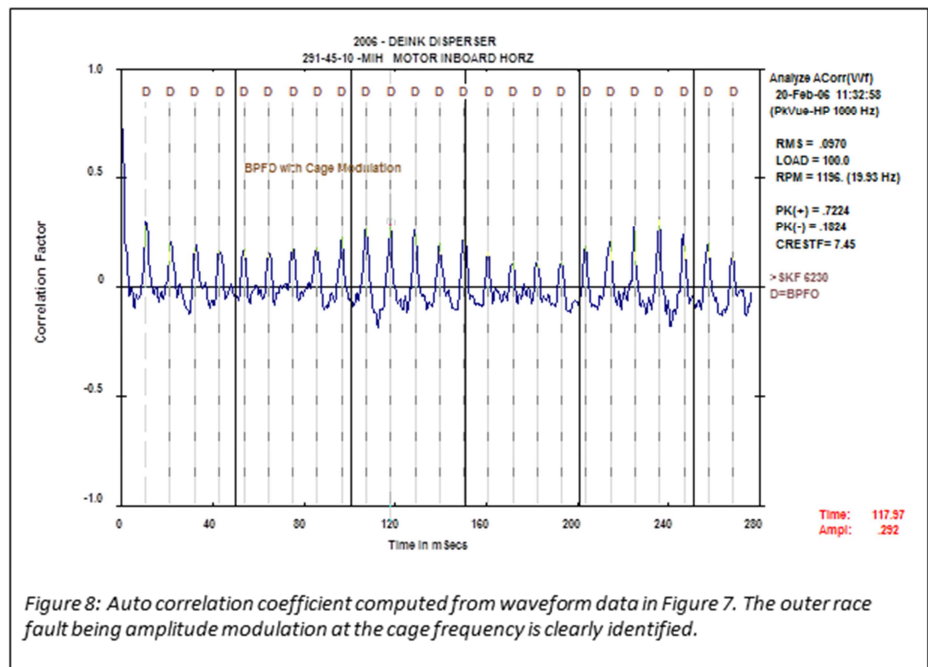


Figure 8: Auto correlation coefficient computed from waveform data in Figure 7. The outer race fault being amplitude modulation at the cage frequency is clearly identified.

are the time intervals corresponding to the time between rollers in the bearing rolling across a defect in the raceway. This bearing has 11 rollers. The peak levels vary in amplitude with the peak value repeating every 11 rollers because, in the case of an outer race remaining stationary and inner race rotating, the BPFO is equal to the number of rollers times the cage frequency. Hence, the outer race faults were being amplitude-modulated at the cage frequency (not the norm). A possible event that may have been occurring would have been a lubrication issue between rollers and the cage. It was recommended to check this as a possible fault by inserting grease into the bearing to see if modulation ceased. Since there were possibly two faults in progress, it was recommended that the surveillance be carried out more frequently (at least weekly) and take corrective action if the peak g-level doubles.

SECTION 3: LIME KILN SECTION CASE STUDY

The routine velocity spectra data acquired from the inboard end of a green liquor pump in the lime kiln section is presented in Figure 9. The primary activity in the velocity spectra data is at running speed and vane pass (5 vanes). The peak g level is 2.5 g's peak-to-peak. There was not an obvious fault in the data presented in Figure 9; however, there was a large audible noise in the headphones. The audible noise triggered the acquisition of band-limited rectified waveform data (1 kHz-40 kHz) employing the PeakVue™ methodology. The resultant spectra and waveform data are presented in Figure 10. There is no or little periodic activity in the spectra data. The peak g level in the high-frequency, band-limited waveform (1 kHz-40 kHz) is 13 g's. The recommended fault level is 10 g's. Due to the lack of any obvious periodic activity in the rectified high-frequency spectra data in Figure 9 and to the high g-level in the waveform data in Figure 10, the suspicion was that of a possible lubrication fault or a high recirculation flow in the pump. To explore this further, the auto correlation coefficient was computed from the waveform in Figure 10. The results are presented in Figure 11. The coefficient data confirmed the noise in the pump was random and hence implied that the source of the noise was probably friction (could have been verified by lubricating the pump). The recommendation was to:

- Monitor more frequently (looking for any rapid growth in g levels).
- Lubricate now if possible.
- Initiate an orderly shutdown and make necessary repairs.

Unfortunately, it was decided to continue operation and the pump suffered catastrophic failure prior to the next scheduled data collection time.

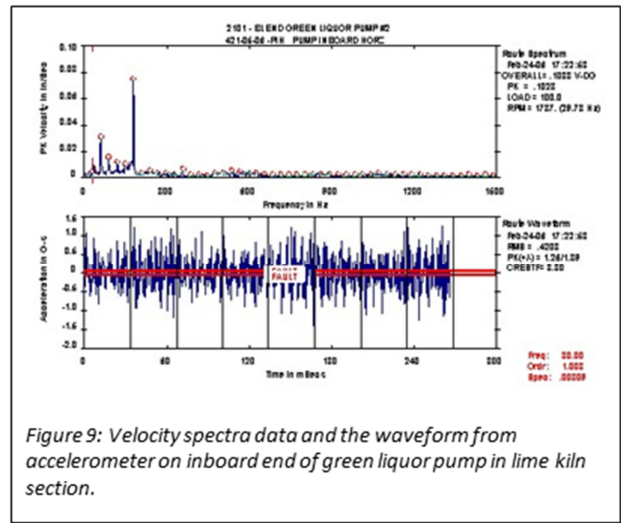


Figure 9: Velocity spectra data and the waveform from accelerometer on inboard end of green liquor pump in lime kiln section.

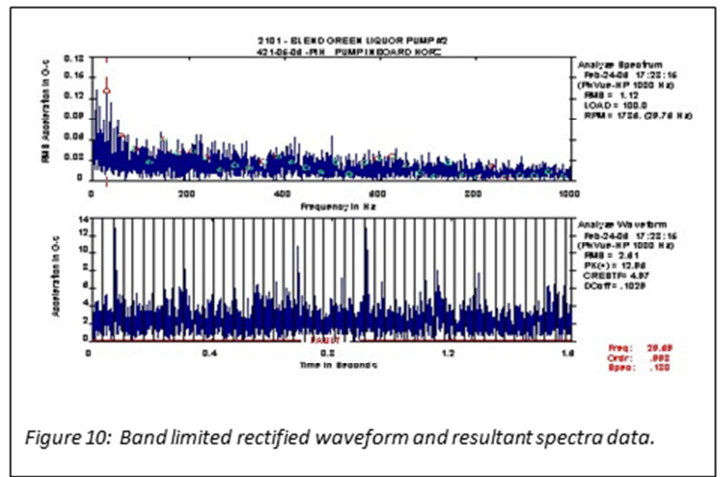


Figure 10: Band limited rectified waveform and resultant spectra data.

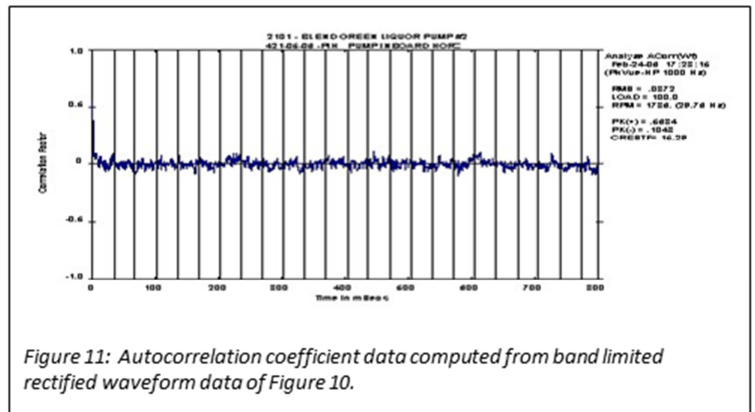


Figure 11: Autocorrelation coefficient data computed from band limited rectified waveform data of Figure 10.

SECTION 4: DIGESTER SECTION CASE STUDY

This case study was taken from the inboard end of a filtrate transfer pump in the digester section. When the routine vibration data was acquired, a loud audible noise was heard in the headphones. This prompted the acquisition of rectified band-limited data (1 kHz-40 kHz). The resultant spectra and waveform data are presented in Figure 12.

The spectra data is showing an inner race fault (BPF1) is present. The waveform data is showing that the peak g level is 80 g's, which is extremely high. The BPF1 fault was being amplitude-modulated (side-banded) at running speed. The 80 g waveform peak levels far exceed the recommended fault level of 10 g's.

To extract the approximate fractional signal level introduced from the periodic BPF1 fault, the autocorrelation coefficient was computed in Figure 13 to extract the largest correlated peak beyond the first few estimates. This value in Figure 13 is 0.284. The square root of 0.284 is 0.53. The fraction of the total signal level due to the periodic activity is 53% or 43 g's. The random activity in the signal was contributing 0% to the correlation coefficient data. Thus, the signal level introduced by non-periodic activity was approximately 37 g's.

Of course, the recommendation for action would be to replace the pump immediately, if possible. The pump experienced catastrophic failure within two days.

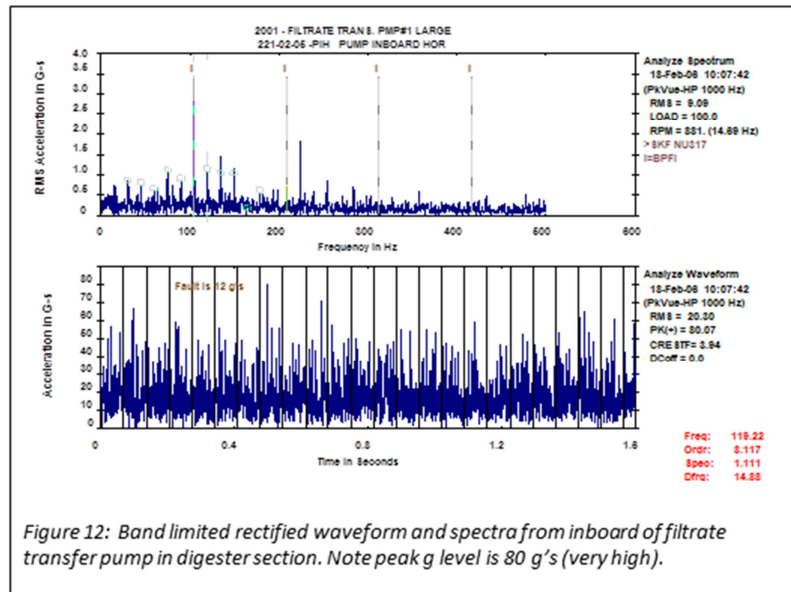


Figure 12: Band limited rectified waveform and spectra from inboard of filtrate transfer pump in digester section. Note peak g level is 80 g's (very high).

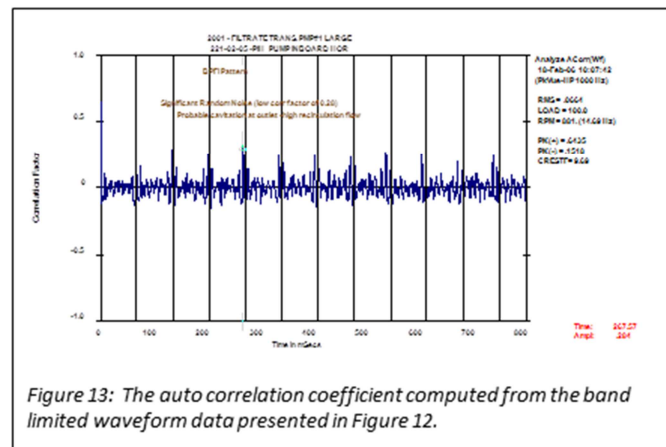


Figure 13: The auto correlation coefficient computed from the band limited waveform data presented in Figure 12.

SECTION 5: PULP MILL SECTION CASE STUDY

Routine vibration monitoring with headphones on an overhung scrubber induced-draft fan triggered the collection of rectified band-limited high-frequency waveform data (1 kHz-40 kHz) presented in Figure 14. The band-limited waveform data had increased from a peak of 1.5 g's to the current 13 g's over the past month. It is not obvious whether any periodic activity is present in the spectra data of Figure 14. The autocorrelation coefficient data computed from the band-limited rectified waveform data in Figure 14 is presented in Figure 15. Here it is obvious there

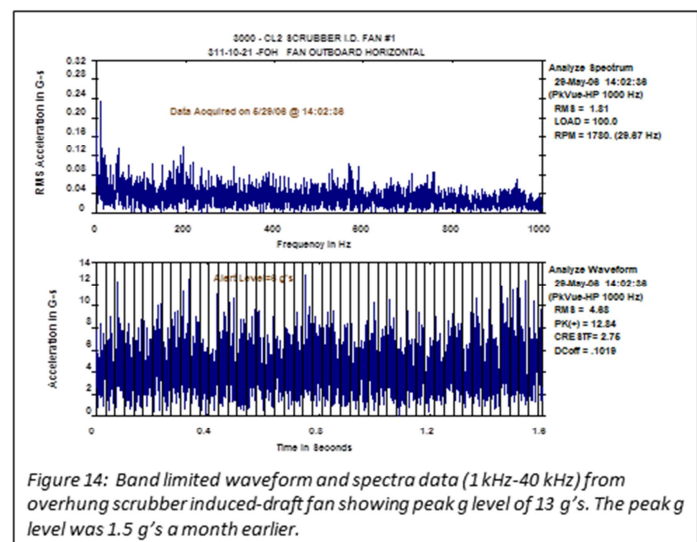


Figure 14: Band limited waveform and spectra data (1 kHz-40 kHz) from overhung scrubber induced-draft fan showing peak g level of 13 g's. The peak g level was 1.5 g's a month earlier.

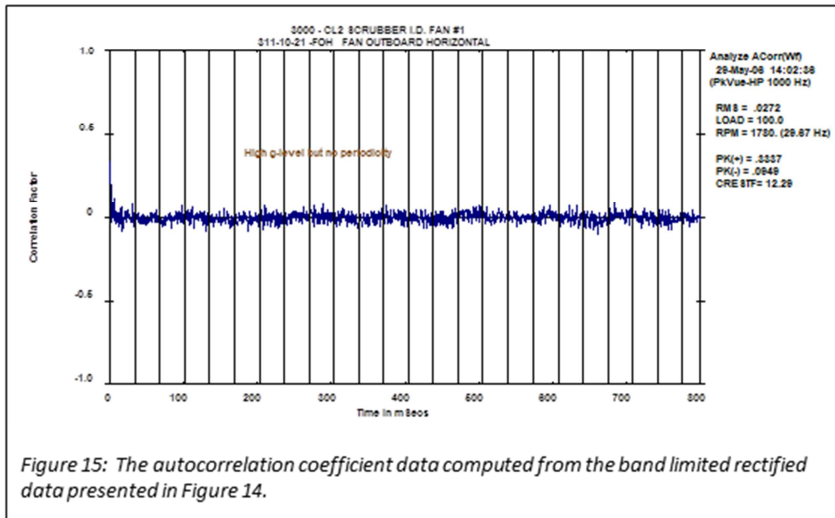


Figure 15: The autocorrelation coefficient data computed from the band limited rectified data presented in Figure 14.

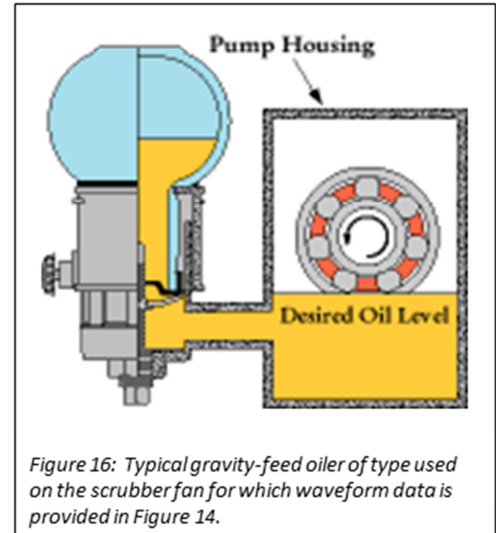


Figure 16: Typical gravity-feed oiler of type used on the scrubber fan for which waveform data is provided in Figure 14.

are no periodic activities in the data presented in Figure 14. A high peak g level occurring randomly suggested a possible lubrication issue was present. This bearing was lubricated with a gravity-feed oiler similar to that shown in Figure 16.

The analyst slightly lifted the oiler bowl to allow some oil to enter into the bearing chamber. The loud noise in the headphones disappeared at that point. Additional band-limited rectified data (1 kHz-40 kHz) was acquired following the addition of oil and presented in Figure 17.

The peak g level decreased from 13 g's to 1.6 g's, which was well below the recommended alert level of 5 g's. As a result, the recommendation was to continue the routine monitoring. It is interesting to note there was an indication of an early-stage BPFO fault starting to present that was not indicated in earlier vibration data (bearing fault assumed to have been introduced while running with the lubrication low).

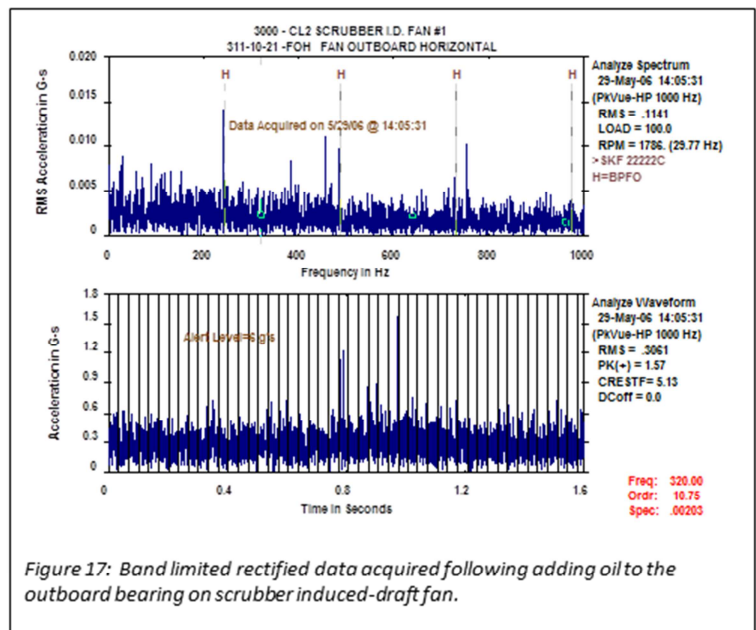


Figure 17: Band limited rectified data acquired following adding oil to the outboard bearing on scrubber induced-draft fan.

SECTION 6: PAPER MACHINE SECTION CASE STUDIES

Case Study 1: Routine audible headphone monitoring on a press section suction roll yielded a clicking noise that faded in and out on a seemingly periodic rate. The velocity spectral data showed no hint of a problem but the band-limited time waveform (0 to 200 Hz) showed some possible impacting once per revolution of the press suction roll. The possible activity at running speed and clicking noise initiated the acquisition of rectified band-limited data (0.5 kHz to 40 kHz) that is presented in Figure 18.

The peak g level of the band-limited rectified signal is 4 g's which is greater than the recommended fault level of 3 g's for the 220 RPM press roll. Additionally, the primary activity in the spectra data is at twice the BPFI on this dual roll bearing. Primary impacting at twice the calculated BPFI indicates that the fault spans across the entire race and the two bearing rolls are staggered relative to each other. This suggests the fault may have been a cracked inner race.

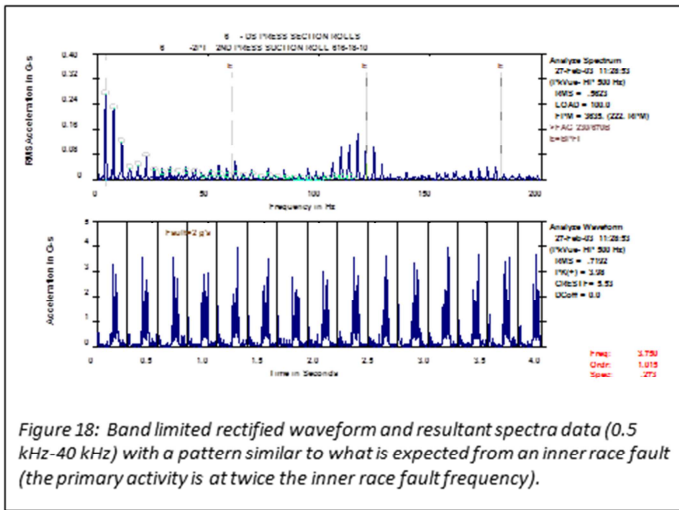


Figure 18: Band limited rectified waveform and resultant spectra data (0.5 kHz-40 kHz) with a pattern similar to what is expected from an inner race fault (the primary activity is at twice the inner race fault frequency).

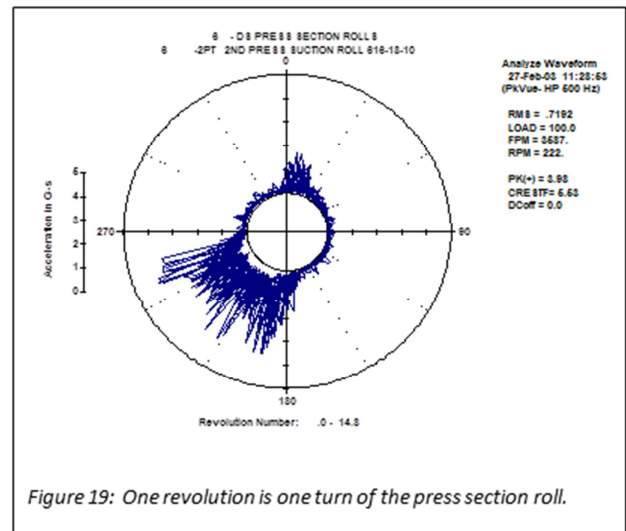


Figure 19: One revolution is one turn of the press section roll.

For additional insight, consider the circular plot where one revolution of the press roll is equal to 360 degrees in the circular plot presented in Figure 19. There are 14.8 revolutions in the band-limited rectified waveform presented in Figure 18 which are all overlaid in Figure 19. There are a grouping of significant impacts in Figure 19 around 220 degrees. There is a less significant grouping of impacting around 20 degrees. These two groupings suggest the press roll experienced two load zones in each roll revolution. The major load zone is around 220 degrees and the minor load zone is around 20 degrees. One load zone is probably due to the weight of the roll and the second is likely the pulling force of the felt. (The felt wraps around several rolls and is turning at a slow rate).

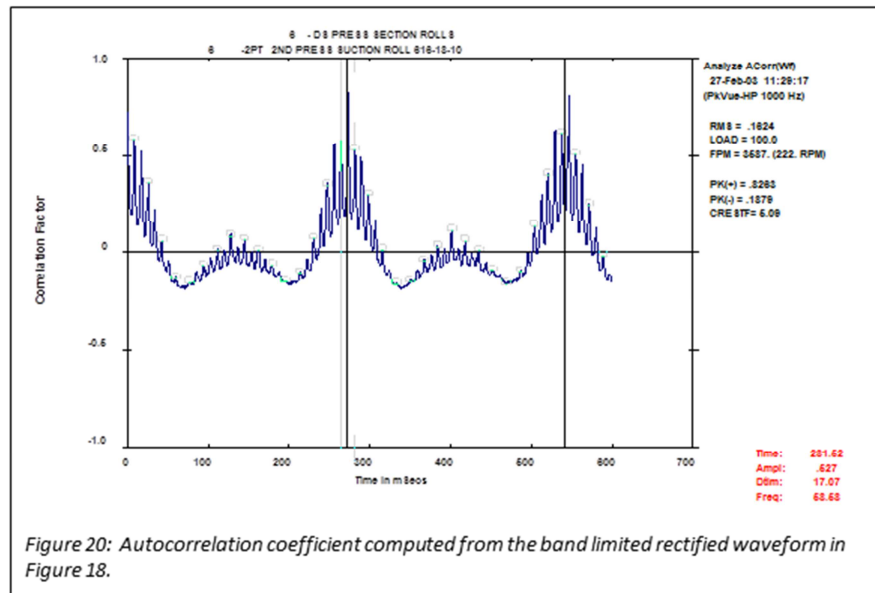


Figure 20: Autocorrelation coefficient computed from the band limited rectified waveform in Figure 18.

The autocorrelation coefficient data computed from the band-limited rectified waveform data in Figure 19 is presented in Figure 20. The time required for the press suction roll to make one revolution was 270 milliseconds. In Figure 20, the peak activity levels (occurring at twice BPFO) are being significantly amplitude-modulated at running speed. There are two regions (one for the major and one for the minor regions identified in Figure 18) where the amplitude modulation at running speed was occurring.

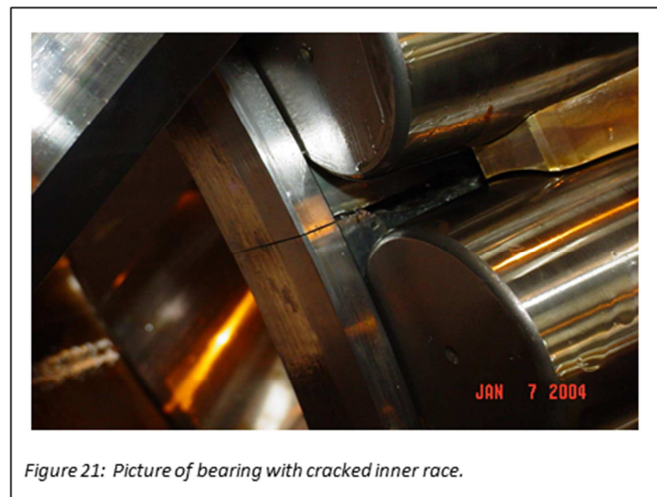


Figure 21: Picture of bearing with cracked inner race.

At about 270 milliseconds in Figure 20, the peak correlation factor is about 0.7. The fraction of the waveform contributed by impacting from the fault is estimated by the square root of 0.7 (0.84) times the peak g level of Figure 18 (4 g's) or 3.4 g's (still greater than the recommended fault level of 3 g's).

The conclusion from the data presented above was that a cracked inner race was possibly present and that data should be acquired on a more frequent schedule to monitor the trend. The next set of vibration data acquired was in 3.5 months, which, in retrospect, was too long of a time duration before additional monitoring. The peak g level had increased from 4 g's to 14 g's. This led to changing the bearing. A picture of the bearing showing the inner race crack is presented in Figure 21. Fortunately, the inner race had not begun to slip on the shaft, which could have caused major damages.

Case Study 2: Due to the importance of finding a cracked inner race before it possibly damages the shaft, a second case is presented where the bearing was replaced early. The roll was located in the dryer section. The bearing was a double roll spherical bearing. It is not known whether the rolls are staggered.

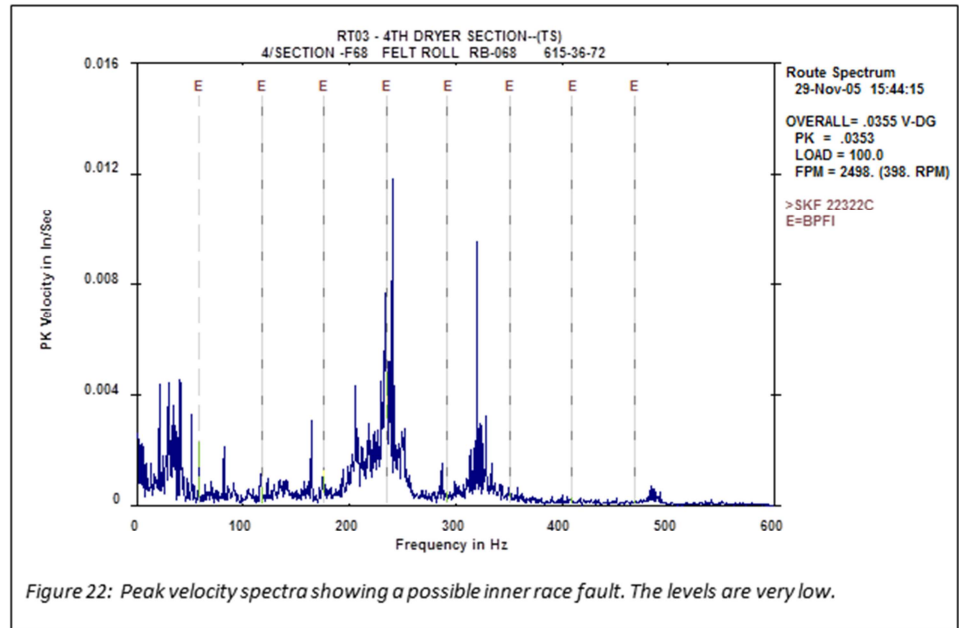


Figure 22: Peak velocity spectra showing a possible inner race fault. The levels are very low.

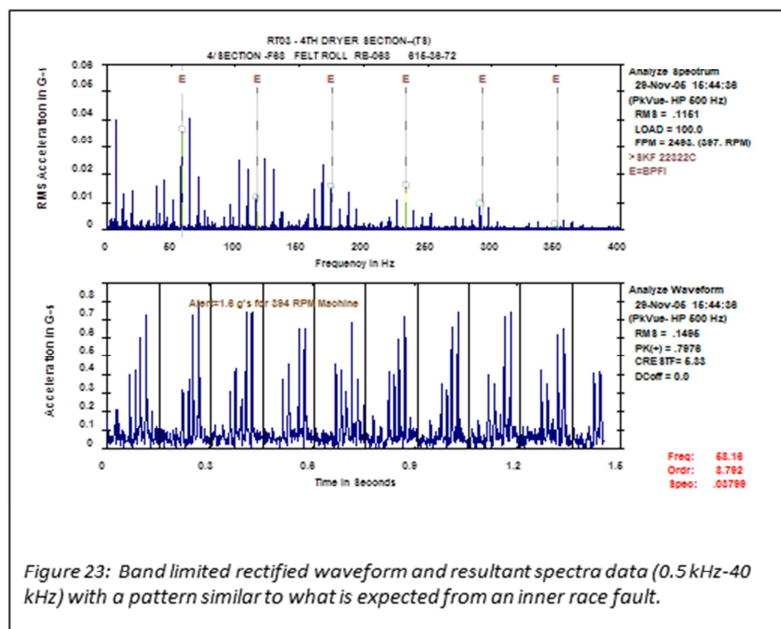


Figure 23: Band limited rectified waveform and resultant spectra data (0.5 kHz-40 kHz) with a pattern similar to what is expected from an inner race fault.

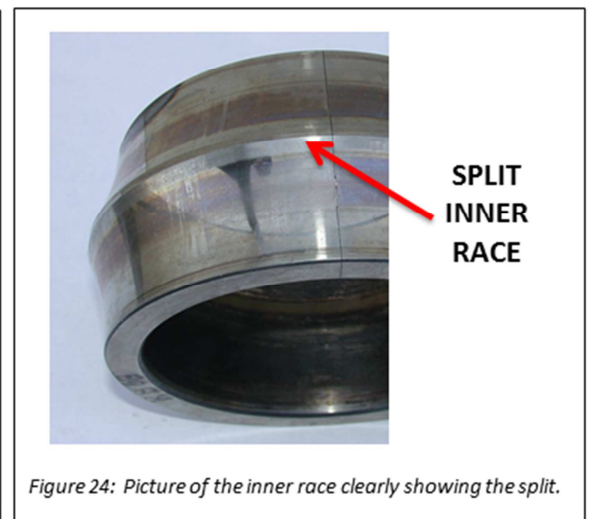


Figure 24: Picture of the inner race clearly showing the split.

The peak velocity spectra data for the dryer section felt roll is presented in Figure 22. The cursor (with harmonics) is set on the BPF1. There is not an indication of an inner race fault in the peak velocity spectra.

The signature in Figure 23 is showing BPF1 being modulated with running speed that is going in and out of the load zone. The peak g level is 0.8 g's, much lower than that recommended 3g alert level for this speed (400 RPM). In Figure 23, the dominant periodic activity is occurring at BPF1, indicating a cracked inner race.

A picture of the inner race of the defective bearing is presented in Figure 24. The inner race is cracked, but the fault had not progressed far (compare the inner race in Figure 24 to the bearing in Figure 21 that had run 3-4 months since fault was first found).

Case Study 3: Audible noise in headphones instigated the acquisition of vibration data on the inboard end of a vacuum pump running at 225 RPM. The peak velocity spectra data was not showing any bearing faults and the acceleration waveform was showing 0.6 g's peak to peak which was not considered of concern. The band-limited rectified waveform and accompanying spectra data (0.5 kHz to 40 kHz) was showing a BPF0 fault on the pump inboard end. The peak g level from the rectified waveform is 4 g's, which is in the early stage fault level, as shown in Figure 25.

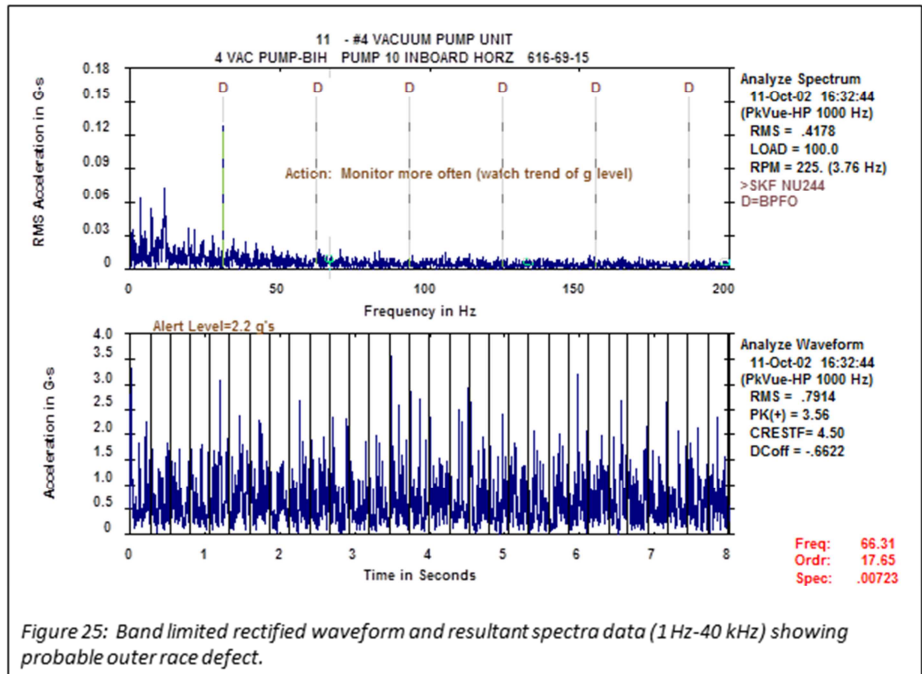


Figure 25: Band limited rectified waveform and resultant spectra data (1 Hz-40 kHz) showing probable outer race defect.

A second set of data was acquired eight months later and the band-limited rectified waveform and resultant spectra are presented in Figure 26. The peak g level had increased from 4 to 26 g's in previous 8 months, which is well beyond the 4 g fault level. There was an extraneous random noise source in addition to the impacting due to the outer race fault. To explore this, the autocorrelation coefficient was computed from the band-limited rectified waveform data in Figure 26 and is presented in Figure 27. The value of the correlation coefficient is about 0.21. To estimate the fraction of the waveform emanating from the periodic activity, the square root of 0.21 was calculated to be .46.

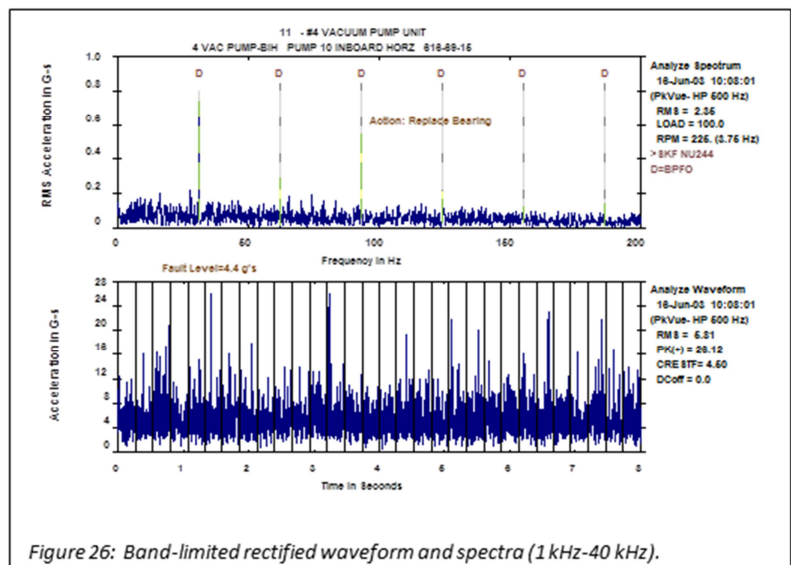


Figure 26: Band-limited rectified waveform and spectra (1 kHz-40 kHz).

Therefore about 46% of the waveform in Figure 26 was from the periodic BPF0 event. The noise (about 14 g's peak) was probably from a well-worn outer race or possibly a lack of lubrication.

Case Study 4: This paper machine had recently undergone an outage where most issues of concern were repaired. The case study presented here is stemming from an alignment issue with the drive-end wire-turning roll. The coupling from the power source to the wire-turning roll was a gear coupler. After the analyst saw the data from the band-limited rectified waveform and corresponding spectra data (0.5 kHz to 40 kHz), his suspicion was there was an alignment problem. He was assured this was not the problem because the coupler was cleaned and repackaged with clean grease during the recent outage. The velocity spectra and acceleration waveform data showed no obvious indication of an alignment problem. The band-limited rectified waveform data (0.5 kHz to 40 kHz) are presented in Figure 28.

In Figure 28, the activity at twice turning speed is significantly greater than the activity at turning speed. This is the signature of a possible alignment problem. The peak g level from Figure 28 is 1.6 g's that is between recommended alert level of 1g and recommended fault level of 2 g's.

To examine this further, the autocorrelation function was computed from the waveform in Figure 28 and presented in Figure 29.

The vertical space bars in Figure 29 are spaced to represent the time required for one revolution (peaks are sharp). There is a rather broad peak approximately midway between the sharp peaks leading to the second harmonic being larger than the first in Figure 28. Further clarification can be gained by examining the circular plot (where one revolution equals 360 degrees) presented in Figure 30.

The impacting is occurring around the 90 degree region and the 310 degree region. The postulate is the outer shell of the coupling was not properly lubricated in sections allowing friction to occur in certain regions. The gear coupling was properly lubricated and the impacting peak g level went from 1.6 g's to 0.17 g's and the activity at twice turning speed disappeared.

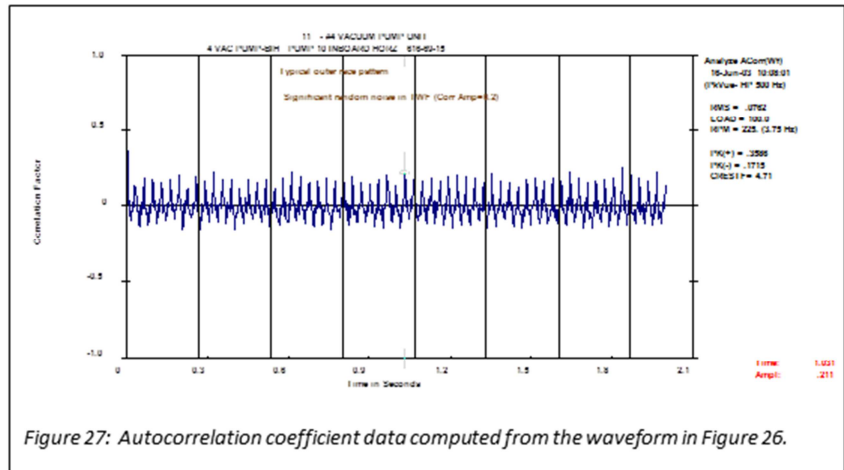


Figure 27: Autocorrelation coefficient data computed from the waveform in Figure 26.

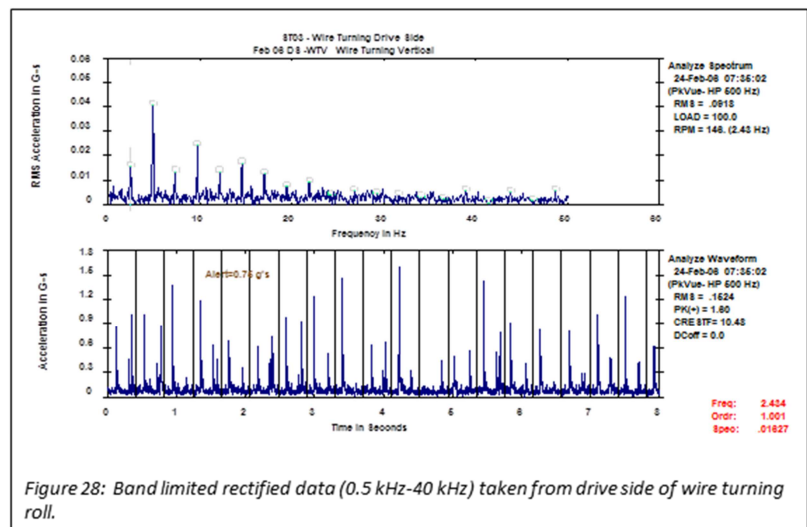


Figure 28: Band limited rectified data (0.5 kHz-40 kHz) taken from drive side of wire turning roll.

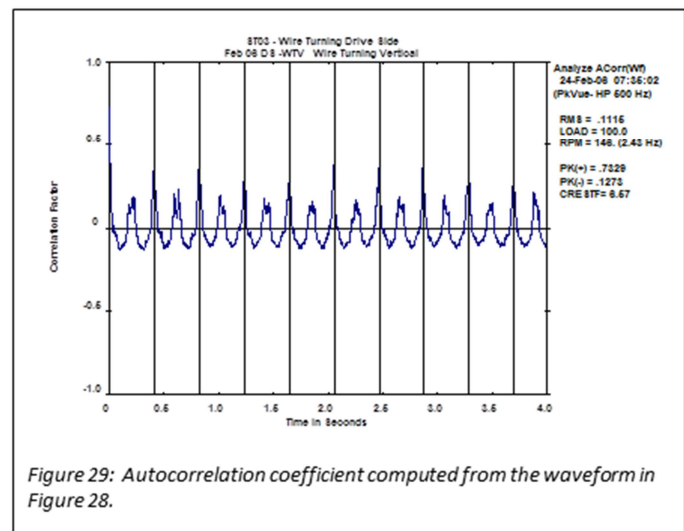


Figure 29: Autocorrelation coefficient computed from the waveform in Figure 28.

Case Study 5: This case study is to demonstrate the detectability of a defective felt by employing the capture of a normal waveform and the implementation of the autocorrelation coefficient function. The caution is the waveform must be of sufficient length (in time) to capture approximately 10-15 revolutions of the felt. Paper machine felts typically rotate in the range of 60 RPM. Therefore, 10-15 seconds of acceleration data having a bandwidth about 0-150 Hz was captured. The acceleration waveform and peak velocity spectra data taken from an accelerometer located on the fourth press section roll are presented in Figure 31.

In Figure 31, the activity in the spectra data in the 50-65 Hz range looks like structure resonance was being excited by a probable defective felt. Also, there was an increase in amplitude in the waveform on a periodic basis of once approximately every five revolutions of the roll. The autocorrelation coefficient computed from the acceleration waveform in Figure 31 is presented in Figure 32. In Figure 32, there was periodic activity occurring every 1.266 seconds (frequency of 0.79 Hz). This corresponds to the felt turning speed (47.4 RPM). The structure resonance was being excited once per revolution of the felt. The recommendation was to replace the felt soon.

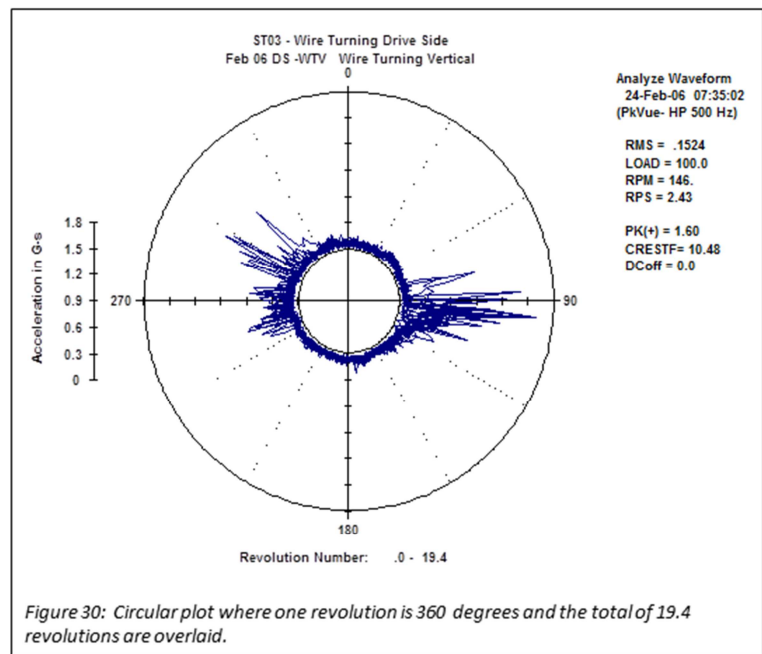


Figure 30: Circular plot where one revolution is 360 degrees and the total of 19.4 revolutions are overlaid.

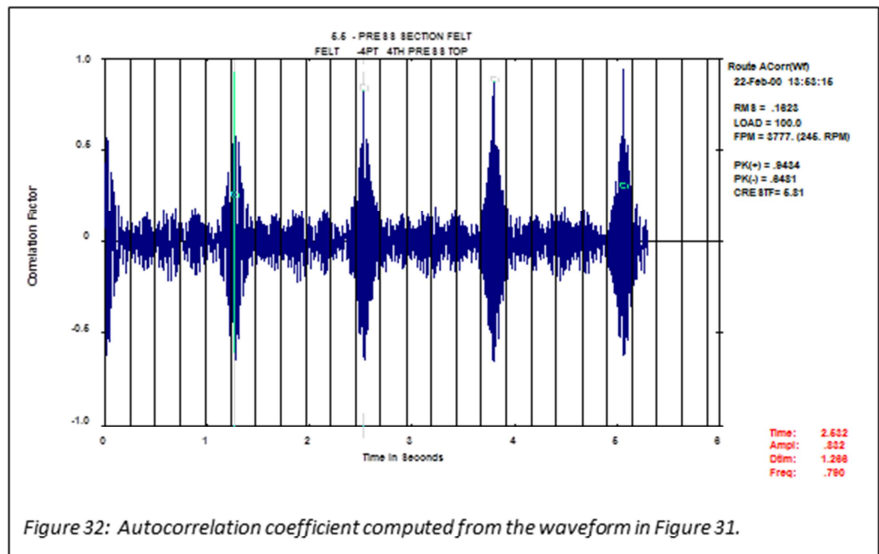


Figure 32: Autocorrelation coefficient computed from the waveform in Figure 31.

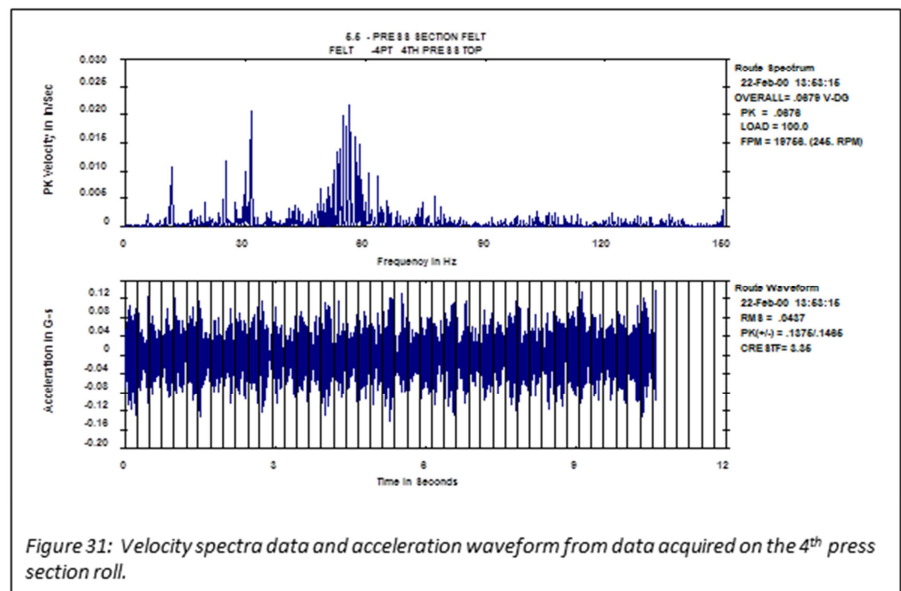


Figure 31: Velocity spectra data and acceleration waveform from data acquired on the 4th press section roll.

SECTION 8: CONCLUSIONS

Several common faults of paper mill machinery were presented in this paper. The objectives were to:

1. Demonstrate a wide variety of fault types.
2. Demonstrate the importance of employing proper accelerometers and analysis tools.

Many faults generate a short burst of stress wave activity (from impacting and friction) that requires sensors responsive up to 15-25 kHz, such as IMI Model 603C01. The sensor frequency response is strongly dependent on how the sensor is attached to the surface of the machine. Accelerometer mounting by stud, by flat magnet on a flat smooth surface and by dual-rail magnet on a curved surface (smooth, rough or painted) were all considered. The conclusion was that the stud-mounting technique was the preferred choice. Mounting the accelerometer with a flat magnet attached to a smooth, flat surface provided sufficient bandwidth for impacting and friction detection. The use of a two-rail magnet on a curved surface would miss several situations where impacting and friction was occurring.

The analysis tools used in this study consisted of the normal spectra data in velocity units and waveform in acceleration units. To cover the high frequency burst of stress waves from impacting, friction and fatiguing, the waveform used was the band-limited rectified signal. The band-limited rectified signal was 0.5-40 kHz, 1.0-40 kHz or 2.0-40 kHz. The rectified waveform was also transformed to spectra data in acceleration units. In addition to waveform and spectra data, the autocorrelation coefficient data was computed from the waveform data graphically displaced. It was a very useful diagnostic tool in both fault identification and severity assessment. Finally, the circular plot data where one revolution of the machine is scaled to become 360 degrees on the circular plot was a very helpful tool.



3425 Walden Avenue, Depew, NY 14043 USA

pcb.com/imi-sensors | imi@pcb.com | 800 959 4464 | +1 716 684 0003

© 2021 PCB Piezotronics - all rights reserved. PCB Piezotronics is a wholly-owned subsidiary of Amphenol Corporation. Endevo is an assumed name of PCB Piezotronics of North Carolina, Inc., which is a wholly-owned subsidiary of PCB Piezotronics, Inc. Accumetrics, Inc. and The Modal Shop, Inc. are wholly-owned subsidiaries of PCB Piezotronics, Inc. IMI Sensors and Larson Davis are Divisions of PCB Piezotronics, Inc. Except for any third party marks for which attribution is provided herein, the company names and product names used in this document may be the registered trademarks or unregistered trademarks of PCB Piezotronics, Inc., PCB Piezotronics of North Carolina, Inc. (d/b/a Endevo), The Modal Shop, Inc. or Accumetrics, Inc. Detailed trademark ownership information is available at www.pcb.com/trademarkownership.

WPL_80_1121